Cylindrical Probe

The formulation for the cylindrical probe parallels that for the spherical probe with the exception that the normalized continuum limit probe current has been approximated by

$$j_{e,0} = K_e[(1 + \tau)/\tau]/\ln(l/r_p x_0) \quad (6)$$

to remain consistent with the Kirchhoff-Peterson-Talbot[5] results. In the collisionless limit Laframboise's numerical results for cylindrical probes collecting monoenergetic electrons may be closely reproduced by

$$j_{e,\infty} = f_c(\tau)(\chi_p/\tau\chi_c)^{\alpha_c} \quad (7)$$

provided $f_c(\tau)$ is defined as

$$f_c(\tau) \equiv (4/\pi)^{1/2}\left(\frac{\pi}{4} - \chi_c\right)^{1/2}$$

Representative values of $f_c(\tau)$ are given in Table 1, α_c is shown on Fig. 2 and $\chi_c = -(\ln 2)/\tau$. It follows that the potential distribution in the region $z_c \leq z \leq 1$ may be approximated by

$$j_{e,\infty} z = f_c(\tau)(\chi/\chi_c)^{\beta_c} \quad (8)$$

where

$$\beta_c = \alpha_c[1 - \ln\tau/\ln(\chi_p/\chi_c)] \quad (9)$$

and, the inner integral is then

$$J_{e,\infty}^{(2)} = \beta_c[E_1(\chi_c) - E_1(\chi_p)] \quad (10)$$

The electron current attracted to a cylindrical probe operating in the transition regime is then

$$j_{e,\infty}/j_e = 1 + (1 + K_e)^{-1}\{G_1(\tau)j_{e,\infty}^{1/2} + j_{e,\infty}\beta_c[E_1(\chi_c) - E_1(\chi_p)]\} + j_{e,\infty}K_e^{-1}(1 + K_e)^{-1}(1 + \tau^{-1})^{-1}\ln(l/r_p X_0) \quad (11)$$

where $j_{e,\infty}$ is the normalized value for the cylindrical probe current in the collisionless limit.

Results and Discussion

The collisional effects were generally found to become more severe as the relative thermal energy of the collected species increased. For example at large values of τ and χ_p, the normalized cylindrical probe electron current density is significantly less than the normalized ion current density when $K_e < 10$.

Typical values of the cylindrical probe electron current are shown in Fig. 3 for values of $\chi_p = |\chi_f| + 10$ where χ_f is the probe floating potential. No solution exists for the current collected by a cylindrical probe operating in the continuum limit and the expression used here is just an approximation. The results for the cylindrical probe are, therefore, thought to be most accurate for large Knudsen numbers and should be used with caution for small K where the solution is dominated by the continuum limit value for the probe current.

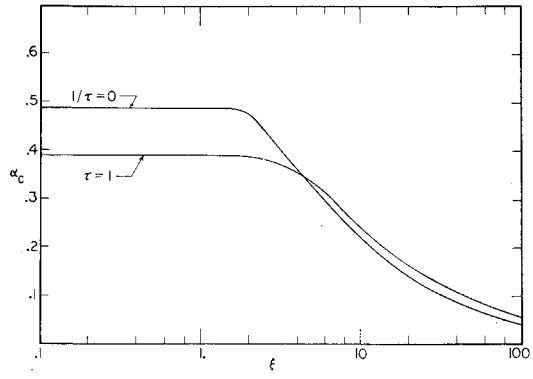

Fig. 2 Correlation exponent for electron collection by a cylindrical probe.

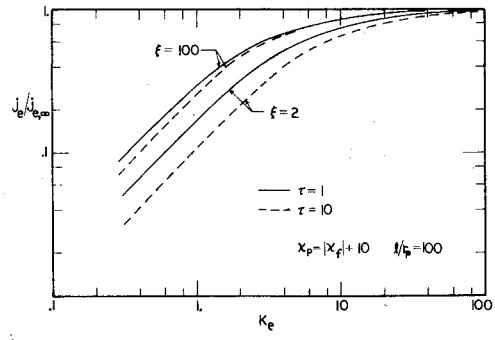

Fig. 3 Cylindrical probe electron current in the transition region.

References

[1] Talbot, L. and Chou, Y. S., "Langmuir Probe Response in the Transition Regime," *Rarefied Gas Dynamics*, edited by C. L. Brundin, Vol. II, Academic Press, New York, 1969, pp. 1723–1737.

[2] Chou, Y. S., Talbot, L., and Willis, D. R., "Kinetic Theory of a Spherical Electrostatic Probe in a Stationary Weakly Ionized Plasma," *The Physics of Fluids*, Vol. 9, 1966, p. 2150.

[3] Kaegi, E. W. and Chin, R., "Stagnation Region Shock Layer Ionization Measurements in Hypersonic Air Flows," AIAA Paper 66-167, Monterey, Calif., 1966.

[4] Dunn, M. G. and Lordi, J. A., "Measurements of Electron Temperature and Number Density in Shock Tunnel Flows, Part I Development of Free-Molecular Langmuire Probes," *AIAA Journal*, Vol. 7, 1969, p. 1958.

[5] Kirchhoff, R. H., Peterson, E. W., and Talbot, L., "An Experimental Study of the Cylindrical Langmuir Probe Response in the Transition Regime," AIAA Paper 70-85, New York, 1970.

[6] Bernstein, I. B. and Rabinowitz, I. N., "Theory of Electrostatic Probes in a Low Density Plasma," *The Physics of Fluids*, Vol. 2, 1959, p. 112.

[7] Laframboise, J. G., "Theory of Spherical and Cylindrical Langmuir Probes in a Collisionless Plasma at Rest," *Rarefied Gas Dynamics*, edited by J. H. de Leeuw, Vol. II, Academic Press, New York, 1966, pp. 22–44.

[8] Su, C. H. and Lam, S. H., "Continuum Theory of Spherical Electrostatic Probes," *The Physics of Fluids*, Vol. 6, 1963, p. 1479.

[9] Cohen, I. M., "Asymptotic Theory of Spherical Electrostatic Probes in a Slightly Ionized, Collision-Dominated Gas," *The Physics of Fluids*, Vol. 6, 1963, p. 1492.

Some Measurement in Pipe Flow

B. Bose*

Jadavpur University, Calcutta-32, India

In semibounded or in-bounded flow, the structure of turbulence largely depends on the properties of the so-called viscous layer in the vicinity of the boundary. The observations of Kline and co-workers[1,2] in turbulent boundary layers have shown some interesting features contradicting the widely accepted model of the viscous sublayer which has been well-known for some time. The salient features of the previous postulation are that the so-called viscous sublayer close to the wall is three-dimensional and is dominated by vigorous bursts

Received September 15, 1970; revision received November 9, 1970.

*Reader, Mechanical Engineering Department.

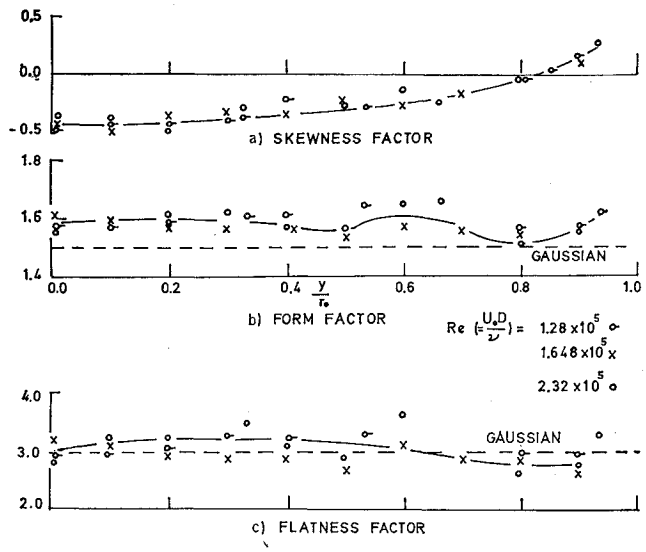

Fig. 1 Distribution of the characteristics of the turbulent signal.

which move away from the boundary and play a major role in the mechanism of mixing and transfer.

Laufer's[3] measurements of fully developed pipe flow, probably the earliest successful measurements in bounded flow, give an over-all description of the flow. They formed the basis of later studies in pipe flow. The recent investigations of Morrison[4] and Coantic[5] in fully developed pipe flow require special mention here. From the hot-wire measurements, these authors supported Kline's model of the so-called viscous layers adjacent to the wall. The present Note is intended to include some new observations in fully developed pipe flow that may be helpful to our understanding of turbulent shear flow, particularly in the light of recent thinking about the structure of turbulence. The experimental details have been described elsewhere.[6]

Characteristics of Turbulent Signals

It is reasonable to analyze the characteristics of the random turbulent signals obtained from a hot-wire, and statistical parameters are obviously the logical choice. The probability density function $p(v)$, which gives information on the amplitude domain of the signals, is defined as the probability of finding a signal between the limits $(v + dv)$ and v. It is a measure of the time spent by the signal in the said interval. The normalized probability density function is defined by

$$\int_{-\infty}^{\infty} p(v)dv = 1 \qquad (1)$$

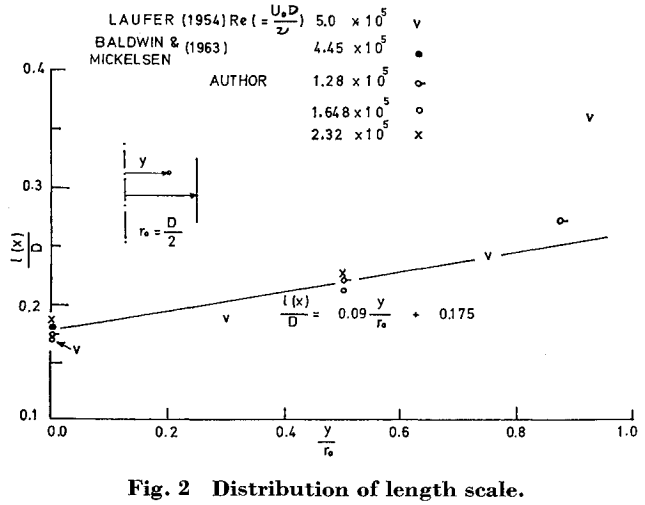

Fig. 2 Distribution of length scale.

Table 1 Estimation of length scale in pipe flow

Author(s)	Reynolds number ($= U_0D/\nu$)	Method of estimating the length scale
Laufer	5.0×10^5	Extrapolating frequency spectra using Eq. (3)
Baldwin and Mickelsen	4.45×10^5	Auto-correlation measurement using Taylor's hypothesis
Author	$1.28\text{–}2.32 \times 10^5$	Extrapolating frequency spectra using Eq. (3); auto-correlation measurement using Taylor's hypothesis

The shape of the probability distribution is described by its moment about the mean, and the nth moment about the mean is given by

$$\langle v^n \rangle = \int_{-\infty}^{\infty} v^n(p)vdv \qquad (2)$$

The distribution of the second moment and the normalized third and fourth moments, better known respectively as form factor, skewness factor, and flatness factor, have been illustrated in Fig. 1 across the radial distance. The results show independency of Reynolds number ($Re = U_0D/\nu$) and indicate a non-Gaussian character of the signals across the pipe section except at a distance $y/r_0 \doteq 0.83$ from the pipe axis. The skewness factor has a high negative value in the core region and changes to a positive value beyond $y/r_0 > 0.83$. It is interesting to note that the form factors of the signals that are directly related to the intensity of fluctuations are higher than the Gaussian value, i.e., $\pi/2$, whereas the flatness factors exhibit a near Gaussian value with a tendency to increase along with skewness factor beyond $y/r_0 > 0.83$. Similar measurements made earlier in free shear layers[7,8] and in uniform flow behind grids[8] also show non-Gaussian distribution of turbulent signals. Again, the skewness factors measured by different investigators[2] in turbulent boundary layers under different pressure gradients indicate a zero skewness at a distance $y^+ \doteq 15[y^+ \doteq (r_0 - y)u_*/\nu$, where u_* is the friction velocity and ν is the kinematic viscosity] from the wall; beyond this value (i.e., $y^+ > 15$), the skewness factors attain a nearly steady value at minus one, and in the region $y^+ < 15$, the skewness factors tend to rise to very high positive values. The bursts or disturbances observed in turbulent boundary layers usually originate in this region.[1,2] In a pipe flow, a zero skewness factor is noticed at $y^+ \doteq 317$, the characteristic of the signals is nearly Gaussian in this region (i.e., at $y^+ \doteq 317$). For the lack of data, this cannot be said for boundary layers.

Eddy Scale

A widely accepted method of specifying a turbulent field is referring to the integral scale, usually called the scale of turbulent eddies, obtained from correlation measurements—space or auto-correlation depending on practical feasibility. Alternately, estimation of scale $1(x)$, by extrapolating spectral measurements, is used sometimes. It has been shown[8] that the integral scale $1(x)$ is directly proportional to the scale of the energy containing eddies λ, that is,

$$1(x) = \lambda/1.13 \qquad (3)$$

where λ is estimated by extrapolating the turn-over frequency of the measured spectra. In case of pipe flow, two-wire correlation measurements are sometimes difficult. The scales $1(x)$, estimated from auto-correlation measurements and using the above relation [Eq. (3)], are plotted in Fig. 2. The results show similarity and Reynolds number independency and compare well with the results obtained extrapolating earlier measurements.[3,9] The particulars of estimating procedure of the preceding results are detailed in Table 1. The scatter of

points (Fig. 2) is probably due to the limitation of using mean local velocity rather than the convection velocity of the turbulent eddies[8] in estimating the length scale using Taylor's hypothesis. The scale of the eddies increases at a very slow rate with radial position

$$1(x) = 0.09(y/r_0) + 0.172 \quad (4)$$

across the considerable portion of pipe section. This rate deviates to a much larger value beyond $y/r_0 > 0.85$. It is unfortunate that the measurements are not extended to the so-called viscous layers. The trend, however, shows that the eddies are elongated near the wall, which is in agreement with the postulation of Townsend[10] and measurements of others.[4,5]

Discussion

The results indicate the dominance of large-scale motions in the wall region of the pipe. As the eddies are stretched more and more due to the presence of the wall, the skewness and flatness factors of the probability distributions tend to increase to high values compared to the Gaussian distributions. The convection velocities of these large-scale motions are also very high compared to the mean local velocity.[4] This is probably a result of the prominance of the three-dimensional disturbances in the wall region.

Earlier investigators indicated resemblance between the turbulent characteristics in the wall region of a pipe flow and that of boundary layer, though the physical constraints of the two flows are different. In boundary-layer flow, one finds a sharp interface between turbulent and nonturbulent regions that implies intermittency, whereas a developed pipe flow is characterized by the absence of intermittency. A significant deviation in the characteristics of the turbulent signals between these two cases, which are logically related to the physics of the flow, is also noticed. It appears that the detailed structure and mechanism of the motion in these two flows would be different. Thus, it is not fully understood that Kline's model of turbulent structure in the boundary layer may be strictly postulated in the pipe flow. A further study to this end seems to be useful.

References

[1] Kline, S. J. et al., "The Structure of Turbulent Boundary Layers," *Journal of Fluid Mechanics*, Vol. 30, 1967, pp. 741–773.

[2] Kline, S. J., "Observed Structure Features in Turbulent and Transitional Boundary Layers," *Proceedings of the Symposium on Fluid Mechanics of Internal Flow*, edited by G. Sovren, Elsevier, New York, 1967, pp. 27–79.

[3] Laufer, J., "The Structure of Turbulence in a Fully Developed Pipe Flow," Rept. 1174, 1954, NACA.

[4] Morrison, W. R. W., "The Structure of Turbulence in Fully Developed Pipe Flow," Research reports, 1967, Univ. of Queensland, Brisbane, Australia.

[5] Coantic, M., "A Study of Pipe Flow and Structure of its Viscous Sub-layer," presented at the IV Euromech Colloquium: The Structure of Turbulence, Southampton Univ., England, March 29–31, 1967.

[6] Bose, B., "Calibration of a Yawed Hot-wire in an Unsteady Flow," *Journal of the Institute of Engineers* (India), Vol. 50, No. 1, Pt. MEI, 1969, pp. 32–37.

[7] Davies, P. O. A. L., "Turbulence Structure in Free Shear Layers," *AIAA Journal*, Vol. 14, No. 11, Nov. 1966, pp. 1971–1978.

[8] Bose, B., "Experimental Study of the Wave Like Characteristics of Turbulence in Free Shear Layers and Flow behind Grids," Ph.D. thesis, 1968, Southampton Univ., England.

[9] Baldwin, L. V. and Mickelson, W. R., "Turbulent Diffusion and Anemometer Measurements," *Transaction of the American Society of Civil Engineers*, Vol. 128, Pt. 1, 1963, pp. 1595–1631.

[10] Townsend, A. A., *The Structure of Turbulent Shear Flow*, Cambridge University Press, Cambridge, England, 1956, Chap. 9, pp. 194–223.

Some Characteristics of Laminated Filamentary Composites

K. S. Chu*

General Dynamics Corporation, Fort Worth, Texas

In a recent design of a certain component of an advanced aircraft, laminated composite material was used for the cover skin. The material was arranged in such a way that 40% of the filaments lies in the direction of a reference axis. The other 60% lies in the $\pm 45°$ directions symmetric to the reference axis. The material is macroscopically orthotropic with its major principal axis oriented in the direction of the reference axis for maximum efficiency. It was rather surprising to observe that the direction of maximum Young's modulus does not coincide with that of the major principal axis. This note is to review the mechanics of the orthotropic materials and to determine the relationship between the independent variables, namely, E_1, E_2, G_{12}, ν_{12} and θ (for notations see Ref. 1) which would cause the seemingly improbable phenomenon to occur.

The basic stress-strain relationship of the orthotropic material is

$$\begin{Bmatrix} \epsilon_1 \\ \epsilon_2 \\ \frac{\gamma_{12}}{2} \end{Bmatrix} = \begin{bmatrix} \frac{1}{E_1} & -\frac{\nu_{21}}{E_2} & 0 \\ -\frac{\nu_{12}}{E_1} & \frac{1}{E_2} & 0 \\ 0 & 0 & \frac{1}{2G_{12}} \end{bmatrix} \begin{Bmatrix} \sigma_2 \\ \sigma_2 \\ \tau_{12} \end{Bmatrix} \quad (1)$$

or

$$\epsilon_{12} = S_{12}\sigma_{12} \quad (2)$$

where the subscripts 1 and 2 indicate the directions of the major and minor principal axes. For other mutually perpendicular directions x and y which do not coincide with directions 1 and 2, the stress-strain relationships are

$$\epsilon_{xy} = S_{xy}\sigma_{xy} \quad (3)$$

and S_{xy} may be obtained by following transformation

$$S_{xy} = T^{-1}S_{12}T \quad (4)$$

where

$$T = \begin{bmatrix} \cos^2\theta & \sin^2\theta & \sin 2\theta \\ \sin^2\theta & \cos^2\theta & -\sin 2\theta \\ -\frac{1}{2}\sin 2\theta & \frac{1}{2}\sin 2\theta & \cos 2\theta \end{bmatrix} \quad (5)$$

Equation (3) may be expressed in the following manner:

$$\begin{Bmatrix} \epsilon_x \\ \epsilon_y \\ \frac{\gamma_{xy}}{2} \end{Bmatrix} = \begin{bmatrix} \frac{1}{E_x} & -\frac{\nu_{yx}}{E_y} & -\frac{m_x}{E_1} \\ -\frac{\nu_{xy}}{E_x} & \frac{1}{E_y} & -\frac{m_y}{E_1} \\ -\frac{m_x}{E_1} & -\frac{m_y}{E_1} & \frac{1}{2G_{xy}} \end{bmatrix} \begin{Bmatrix} \sigma_x \\ \sigma_y \\ \tau_{xy} \end{Bmatrix} \quad (6)$$

Since we are interested in the relationship between E_x and the independent variables: E_1, E_2, G_{12} and ν_{12}, the expansion of Eq. (4) yields

$$\frac{E_1}{E_x} = \cos^4\theta + \frac{E_1}{E_2}\sin^4\theta + \frac{1}{4}\left(\frac{E_1}{G_{12}} - 2\nu_{12}\right)\sin^2 2\theta \quad (7)$$

Received October 4, 1970; revision received March 9, 1971.

* Senior Structures Engineer, Advanced Structural Dynamics, Convair Aerospace Division.